Free-carrier transport in superlattices: Smooth transition between the quasi-two-dimensional and uniform three-dimensional limits

J. R. Meyer, D. J. Arnold,* C. A. Hoffman, and F. J. Bartoli
Naval Research Laboratory, Washington, D.C. 20375
(Received 14 August 1991)

Presented here is a comprehensive, single-particle formalism for free-carrier transport in semiconductor superlattices with cylindrically symmetric energy dispersion. The spatial nonuniformity of the carrier population is accounted for by employing a scattering potential that is weighted by the wave-function distribution function. In the limit of large barrier-to-well thickness ratios, one regains the quasi-two-dimensional (2D) expressions derived previously. In the opposite limit of thin barriers and hence a nearly uniform wave-function distribution, transport in the superlattice becomes analogous to that in a 3D semiconductor with an anisotropic effective mass. Anisotropic relaxation times are obtained for acoustic-phonon, nonpolar-optical-phonon, polar-optical-phonon, and ionized-impurity scattering. Arbitrary energy dispersion relations are assumed, so that complex, numerically derived band structures may be straightforwardly incorporated. For the example of a HgTe-CdTe superlattice with weak hole dispersion but relatively strong electron dispersion in the growth direction, superlattice mobilities obtained using the present formalism are compared in detail with results for the quasi-2D and isotropic 3D limits.

I. INTRODUCTION

The past 15 years have seen the appearance of numerous theoretical treatments of free-carrier transport in semiconductor heterostructures.[1,2] Nearly all of these have been based on the properties of a quasi-two-dimensional (2D) electron gas. That is, they are appropriate for carriers at heterojunctions, in single quantum wells, or in multiple quantum wells (as long as the barriers are thick enough that interwell tunneling, scattering, and screening are negligible). On the other hand, the case of superlattices, for which interwell effects are significant and the transport is three dimensional, has received surprisingly little attention.[3]

In the present study, we derive a general single-particle formulation of free-carrier transport in semiconductors with modulated wave-function distribution functions $\rho(z) \propto \psi^*(z)\psi(z)$, where $\hat{\mathbf{z}}$ is the growth axis. With it, we can smoothly bridge the two limits that have been treated extensively in previous work: quasi-2D, which is obtained in the multiple quantum well limit, and 3D, which is obtained in the limit of vanishing modulation along the z axis. Superlattices occupy the intermediate region between these two limits, since in general they have both a modulated distribution function and an anisotropic three-dimensional energy dispersion (hence an anisotropic relaxation time). The approach adopted below is based on the intuitively obvious observation that the scattering potential in a nonuniform structure must be weighted by the spatial overlap of the potential with the carrier distribution function. While this consideration is well known from quasi-2D treatments of ionized impurity scattering,[4] it has not to our knowledge been recognized that the same procedure leads straightforwardly to a general method for obtaining transition rates due to both impurity and phonon scattering in the more general superlattice regime. In the multiple quantum well limit, our expressions reproduce the form factors derived previously for quasi-2D transport.[5] In the opposite limit of nearly uniform $\rho(z)$, transport in the superlattice becomes analogous to that in a 3D semiconductor with an anisotropic effective mass.

The present theory can treat arbitrary superlattice band structures, which are incorporated in the form of cylindrically symmetric dispersion relations $E(k_\rho, k_z)$ for the various subbands [$k_\rho = (k_x^2 + k_y^2)^{1/2}$ and k_z are the in-plane and growth direction wave vectors]. Once the generalized transition rates for free-carrier scattering in the superlattice have been determined, least-squares fits for the anisotropic momentum relaxation times $\tau(k_\rho, k_z)$ which best solve the linear Boltzmann equation will be obtained. From the relaxation time for an electric field along either the $\hat{\mathbf{x}}$ or $\hat{\mathbf{z}}$ axis, $[\tau_x(k_\rho, k_z) \neq \tau_z(k_\rho, k_z)]$, either the in-plane or the growth-direction mobility can then be calculated. However, the generalized transition rates are equally applicable to treatments of superlattice transport at high electric fields.

To our knowledge, no previous investigator has explicitly considered in-plane transport for superlattices as a distinct case from the quasi-2D and uniform 3D limits. Artaki and Hess incorporated the anisotropic superlattice dispersion relations into a treatment of energy relaxation processes in GaAs-$Ga_{1-x}Al_xAs$, but they then employed isotropic bulk 3D expressions for the scattering rates.[6] Other workers have considered transport along the $\hat{\mathbf{z}}$ axis of a superlattice. Palmier and Chomette included the anisotropy of the dispersion in a study of growth-direction mobilities, but in order to simplify solution of

the Boltzmann equation they made the drastic approximation of assuming an isotropic relaxation time.[7] Warren and Butcher corrected this deficiency by using an iterative method to solve for $\tau(k_\rho, k_z)$.[8] However, their calculations were effectively carried out in the anisotropic bulk limit, i.e., with anisotropic 3D dispersion relations but with a uniform carrier population. None of these workers have discussed the need for taking into account the nonuniformity of the wave-function distribution function in a superlattice.

The paper is organized as follows. In Sec. II, the weighted potential is derived in terms of the actual potential, and Fermi's golden rule is used to obtain general transition rates for scattering in systems with modulated wave-function distribution functions $\rho(z)$. Section III then considers specific scattering potentials for ionized impurities and for acoustic-, nonpolar-optical-, and polar-optical-phonon modes. A Boltzmann equation approach to calculating electron and hole mobilities in structures with arbitrary dispersion relations is summarized in Sec. IV, and an accurate method for obtaining self-consistent solutions in the anisotropic regime is discussed. For the example of a HgTe-CdTe superlattice with weak hole dispersion but relatively strong electron dispersion in the growth direction, we perform in Sec. V a detailed comparison of mobilities obtained in the quasi-2D, superlattice, and isotropic 3D limits. The importance of properly treating the superlattice mobility is confirmed, since in many cases it is considerably different from either of the two limiting approximations.

II. WEIGHTED POTENTIAL AND TRANSITION RATES IN A SUPERLATTICE

Using Fermi's golden rule, the transition rate for scattering from a state $\mathbf{k}_1$ to a state $\mathbf{k}_2$ due to mechanism Γ may be approximated

$$W_\Gamma(\mathbf{q}) \approx \frac{2\pi}{\hbar}\delta_E \frac{1}{\Omega}\int d^3r_0 N_\Gamma(\mathbf{r_0})|\mathcal{V}^\Gamma(\mathbf{q},\mathbf{r}_0)|^2, \quad (2.1)$$

where $\mathbf{q} \equiv \mathbf{k}_2 - \mathbf{k}_1$, $\delta_E \equiv \delta(E_2 - E_1 \pm \hbar\omega_\Gamma)$, $\pm\hbar\omega_\Gamma$ is the energy transfer for inelastic processes, Ω is the volume of the system, $N_\Gamma(\mathbf{r}_0)$ is the density of scattering centers (which may be a nonuniform function of position $\mathbf{r}_0$), and $\mathcal{V}^\Gamma(\mathbf{q},\mathbf{r}_0)$ is the "weighted" scattering potential (see below). This expression may be used in either 2D or 3D, except that the units of some of the terms depend on dimensionality.[9]

In a uniform 3D system, the weighted potential $\mathcal{V}$ and the actual potential V are equivalent:

$$\mathcal{V}_{3D}(\mathbf{q},\mathbf{r}_0) = \int e^{i\mathbf{q}\cdot\mathbf{r}} V(\mathbf{r}-\mathbf{r}_0)d^3r \rightarrow V(\mathbf{q}), \quad (2.2)$$

which is independent of $\mathbf{r}_0$. In a superlattice with cylindrical symmetry, however, it makes a difference whether the origin of a central potential $V(\mathbf{r}-\mathbf{r}_0)$ lies in a well or a barrier. That is, the actual potential must be weighted by its overlap with the carrier wave-function distribution function: $\mathcal{V}(\mathbf{r},\mathbf{r}_0) = \rho(\mathbf{r})V(\mathbf{r}-\mathbf{r}_0)$. The Fourier transform required for Eq. (2.1) is then

$$\mathcal{V}_{SL}(q_\rho, q_z, z_0) = \Omega\int e^{i\mathbf{q}\cdot\mathbf{r}} V(\mathbf{r}-\mathbf{r}_0)\rho(\mathbf{r})d^3r \rightarrow L\int_{-L/2}^{L/2} e^{iq_z z} V(q_\rho, z, z_0)\rho(z)dz, \quad (2.3)$$

where L is the total thickness of the superlattice (assumed to be much greater than the single-period thickness d), $V(q_\rho, z, z_0)$ is the actual potential, Fourier transformed only in the plane:

$$V(q_\rho, z, z_0) = \frac{1}{2\pi}\int_{-\infty}^{\infty} dq_z' e^{-iq_z'(z-z_0)} V(q_\rho, q_z') \quad (2.4)$$

and the distribution function is uniform in the plane and has been normalized to have unit probability over the entire sample:

$$\int_{-L/2}^{L/2} \rho(z)dz = 1. \quad (2.5)$$

For a many-period superlattice, one is generally concerned about the spatial variation of the potential relative to the periodicity of the wells and barriers, but not with the absolute position z_0 within the structure. It is therefore convenient to place z_0 in the central period of the superlattice and write $z \equiv md + s$, where m is the period index and s varies between $-d/2$ and $d/2$. The relation between the effective potential and the actual potential may then be written

$$\mathcal{V}_{SL}(q_\rho, q_z, z_0) = \frac{d}{2\pi}\sum_{m=-\mathcal{N}_W/2}^{\mathcal{N}_W/2}\int_{-d/2}^{d/2} g(s)ds\int_{-\infty}^{\infty} dq_z' e^{iq_z z - iq_z'(md+s-z_0)} V(q_\rho, q_z'), \quad (2.6)$$

where $\mathcal{N}_W \gg 1$ is the total number of superlattice periods and $g(s)$ is the distribution function for a single period, normalized to unity:

$$\int_{-d/2}^{d/2} g(s)ds = 1, \quad (2.7)$$

i.e., $g(s) = (L/d)\rho(z - md)$ (Sec. V below gives an explicit expression for g in the infinite-square-well approximation). In terms of the weighted potential, the scattering rate is then

$$W^{SL}(q_\rho, q_z) = \frac{2\pi}{\hbar}\delta_E \frac{1}{d}\int_{-L/2}^{L/2} dz_0 N(z_0) \times |\mathcal{V}_{SL}(q_\rho, q_z, z_0)|^2. \quad (2.8)$$

It is easily confirmed that in the uniform limit [$g(s) \rightarrow 1/d$], one regains the actual potential: $\mathcal{V}(q_\rho, q_z, z_0) \rightarrow V(q_\rho, q_z)$ multiplied by an irrelevant phase factor. The scattering rate then has the familiar form

$$W^{3D}(q_\rho, q_z) = \frac{2\pi}{\hbar}\delta_E N |V(q_\rho, q_z)|^2. \tag{2.9}$$

An analogous weighted potential has been employed previously to treat ionized impurity scattering in quasi-2D systems.[4] In that limit, k_z is not a good quantum number and the effective potential depends only on the wave-vector transfer in the plane:

$$\begin{aligned}\mathcal{V}_{2D}(q_\rho, z_0) &= \int_{-L/2}^{L/2} V(q_\rho, z, z_0)\rho(z)dz \\ &= \frac{1}{2\pi}\int_{-L/2}^{L/2}\rho(z)dz\int_{-\infty}^{\infty} dq_z' e^{-iq_z'(z-z_0)} \\ &\quad \times V(q_\rho, q_z')\end{aligned} \tag{2.10}$$

from which

$$W^{2D}(q_\rho) = \frac{2\pi}{\hbar}\delta_E \int_{-L/2}^{L/2} dz_0 N(z_0)|\mathcal{V}_{2D}(q_\rho, z_0)|^2. \tag{2.11}$$

Note that in the multiple-quantum-well (MQW) limit, where the superlattice period d is much longer than both the range of the potential and the localized region where the distribution function is concentrated, the superlattice and quasi-2D weighted potentials are equivalent apart from a multiplicative constant:

$$\mathcal{V}_{MQW}(q_\rho, q_z, z_0) \rightarrow d\mathcal{V}_{2D}(q_\rho, z_0) \tag{2.12}$$

and

$$W^{MQW}(q_\rho, q_z) \rightarrow dW^{2D}(q_\rho). \tag{2.13}$$

On the other hand, if the superlattice period is decreased to the point where interwell interactions become significant, the superlattice and quasi-2D potentials differ qualitatively.

III. SCATTERING MECHANISMS

In the previous section, the Born approximation was used to estimate the transition rate $W(\mathbf{q})$ for scattering by an arbitrary potential $V(\mathbf{q})$, in either a quasi-2D, a uniform 3D, or a nonuniform 3D (superlattice) system. In this section we explicitly consider the effects of dimensionality and uniformity on the scattering rates obtained for four common scattering mechanisms: ionized impurities (II), acoustic phonons (AC), nonpolar optical phonons (NPO), and polar optical phonons (PO).

A. Ionized impurities

Ionized impurity scattering in quasi-2D electron systems has been discussed by Stern and Howard.[4] For the case of inversion-layer electrons in silicon, they solved Poisson's equation to obtain the screened Coulomb potential, explicitly accounting for the nonuniform spatial distribution of the electron wave functions. In generalizing to a superlattice, we must first estimate the density of induced screening electrons as a function of position. In the Thomas-Fermi approximation:

$$\begin{aligned}n_{ind}(\rho, z, z_0) &= \frac{\kappa_0 q_{s2}}{2\pi e^2} g(z - md) \\ &\quad \times \int_{-d/2}^{d/2} g(s_1)V(\rho, z = md + s_1, z_0)ds_1,\end{aligned} \tag{3.1}$$

where κ_0 is the static dielectric constant, m is the index of the superlattice period containing z, $V(\mathbf{r}, z_0)$ is the actual potential, and q_{s2} is the 2D screening wave vector:

$$q_{s2} = \frac{2\pi e^2}{\kappa_0}\frac{\partial n_s}{\partial E_F}. \tag{3.2}$$

Poisson's equation for cylindrical symmetry may then be written

$$\frac{\partial^2 V(q_\rho, z, z_0)}{\partial z^2} - q_\rho^2 V(q_\rho, z, z_0) = \frac{4\pi e^2}{\kappa_0}\delta(z - z_0) + 2q_{s2}g(z - md)\int_{-d/2}^{d/2} g(s_1)V(q_\rho, z = md + s_1, z_0)ds_1, \tag{3.3}$$

where the first term on the right corresponds to the impurity charge and the second represents the induced electron charge.

Potentials derived from Eq. (3.3) are anisotropic because the spatial distribution of the screening charge is highly nonuniform, taking the form of sheets of charge concentrated in the quantum wells. At high carrier concentrations where the 3D screening length q_{s3}^{-1} (see below) is much smaller than the superlattice period d, one expects the quasi-2D result for a single well to be a relatively good approximation. However, at low and intermediate concentrations where $q_{s3}^{-1} \geq d$, it is essential to include both interwell screening and scattering by impurities in remote periods.

A detailed analysis of ionized impurity scattering in multiwell systems will be discussed in a separate work.[10] For the sample calculations discussed in Sec. V, we use a simplified approach which is found to be surprisingly accurate when $q_{s3}^{-1} > d$. Namely, the familiar isotropic 3D screened Coulomb potential has been employed. For lightly-to-moderately doped HgTe-CdTe superlattices ($n \leq 3\times 10^{16}$ cm^{-3}), this approximation leads to less than 5% error when the resulting mobility is compared to the more exact calculation using the anisotropic

potential. We thus use

$$V(q_\rho, q_z) = -\frac{4\pi e^2}{\kappa_0(q_{s3}^2 + q_\rho^2 + q_z^2)}, \tag{3.4}$$

where the 3D screening wave vector is given by

$$q_{s3}^2 = \frac{4\pi e^2}{\kappa_0}\frac{\partial n}{\partial E_F}, \tag{3.5}$$

and in some regions one must sum over contributions by both electrons and holes. The weighted potentials $\mathcal{V}_{\rm SL}$ and $\mathcal{V}_{\rm 2D}$ are then obtained from Eqs. (2.6) and (2.10), and the transition rates from Eqs. (2.8) and (2.11). Note that we have separated the effects of wave-function nonuniformity and 2D vs 3D dispersion from those of the dimensionality of the screening system (which will be discussed in Ref. 10). When quasi-2D, isotropic 3D, and superlattice mobilities are compared in Sec. V, all three calculations will employ the same isotropic screened Coulomb potential. For simplicity, those calculations will assume that the impurities are uniformly distributed throughout the wells and barriers.

B. Acoustic phonons

Whereas ionized impurity scattering involves a stationary scattering center which may occupy either a well or a barrier, the potential for phonon scattering is nonlocalized (ignoring phonon confinement effects). The density of scattering centers in Eq. (2.8) is therefore independent of position. Using Eq. (2.6) and performing the integration over dz_0, we obtain

$$W_{\rm ph}^{\rm SL}(q_\rho, q_z) = \frac{2\pi}{\hbar}\delta(E_2 - E_1 \pm \hbar\omega_{\rm ph})\frac{d}{2\pi} \times \sum_{-\mathcal{N}_W/2}^{\mathcal{N}_W/2}\int_{-d/2}^{d/2} g(s_1)ds_1 \int_{-d/2}^{d/2} g(s_2)ds_2 \int_{-\infty}^{\infty} dq_z' e^{i(q_z'-q_z)(md+s_2-s_1)} N_{\rm ph}(q_\rho, q_z')|V(q_\rho, q_z')|^2, \tag{3.6}$$

where N now appears under the dq_z' integral because for phonon scattering, the matrix element should be considered $[N_{\rm ph}(\mathbf{q})]^{1/2}V(\mathbf{q})$ (if V is the potential due to a single phonon).[11]

For the case of acoustic mode scattering in the elastic limit ($\hbar\omega_{\rm ph} \to 0$), one has[11]

$$N(\mathbf{q})|V(\mathbf{q})|^2 = \frac{\hbar}{2\pi}\frac{k_B T \Xi^2}{\rho v_s^2}, \tag{3.7}$$

where Ξ is the acoustic deformation potential, ρ is the mass density, and v_s is the longitudinal sound velocity. Substitution into Eq. (3.6) then yields

$$W_{\rm AC}^{\rm SL}(q_\rho, q_z) = W_{\rm AC}^{\rm 3D}\left(d\int_{-d/2}^{d/2} g^2(s_1)ds_1\right), \tag{3.8}$$

where the familiar result for a uniform 3D system [$g(s) \to d^{-1}$] is

$$W_{\rm AC}^{\rm 3D}(q_\rho, q_z) = \frac{k_B T \Xi^2}{\rho v_s^2}\delta(E_2 - E_1), \tag{3.9}$$

which is independent of $\mathbf{q}$.

It is easily shown that one regains Eq. (2.13) in the multiple quantum well limit [$g(\pm d/2) \to 0$]. The quasi-2D result,

$$W_{\rm AC}^{\rm 2D}(q_\rho, q_z) = W_{\rm AC}^{\rm 3D}\left(\int_{-L/2}^{L/2}\rho^2(z_1)dz_1\right), \tag{3.10}$$

agrees with that obtained previously by Price,[5] who incorporated form factors to account for momentum transfer in the $\hat{\mathbf{z}}$ direction.

C. Nonpolar optical phonons

As in the case of acoustic modes, the matrix element for nonpolar optical phonons is independent of $\mathbf{q}$ in lowest order. Dimensionality effects on the transition rates are therefore exactly analogous, and Eqs. (3.8) and (3.10) still hold if AC is replaced by NPO. It is necessary only to specify the uniform 3D result:[11]

$$W_{\rm NPO}^{\rm 3D}(q_\rho, q_z) = \sum_{\pm}\frac{\pi D^2}{\rho\omega_{\rm op}}(N_{\rm op} + \tfrac{1}{2} \pm \tfrac{1}{2}) \times\delta(E_2 - E_1 \pm \hbar\omega_{\rm op}), \tag{3.11}$$

where D is the optical deformation potential, $\omega_{\rm op}$ is the optical-phonon frequency, the sum is over phonon emission and absorption processes, and

$$N_{\rm op} = \frac{1}{e^{\hbar\omega_{\rm op}/k_B T} - 1}. \tag{3.12}$$

Nonpolar optical scattering in the quasi-2D limit has been discussed previously by Ridley.[12]

D. Polar optical phonons

For polar-optical-phonon scattering, one obtains, using the Frölich Hamiltonian,

$$N|V|^2 = \sum_{\pm}(N_{\rm op} + \tfrac{1}{2} \pm \tfrac{1}{2})\frac{2\pi\hbar\omega_{\rm op}e^2}{q^2}\left(\frac{1}{\kappa_\infty} - \frac{1}{\kappa_0}\right), \tag{3.13}$$

where κ_∞ is the high-frequency dielectric constant, we have neglected screening, and $N_{\rm op}$ from Eq. (3.12) is in-

dependent of $\mathbf{q}$. Inserting Eq. (3.13) into Eq. (3.6), we obtain

$$W_{\mathrm{PO}}^{\mathrm{SL}}(q_\rho, q_z) = W_{\mathrm{PO}}^{\mathrm{3D}}(q_\rho, q_z) G_{\mathrm{SL}}(q_\rho, q_z), \tag{3.14}$$

where the uniform 3D transition rate for polar optical phonons is[11]

$$W_{\mathrm{PO}}^{\mathrm{3D}}(q_\rho, q_z) = \sum_{\pm} (N_{\mathrm{op}} + \tfrac{1}{2} \pm \tfrac{1}{2}) \frac{4\pi^2 e^2 \omega_{\mathrm{op}}}{(q_\rho^2 + q_z^2)} \times \left(\frac{1}{\kappa_\infty} - \frac{1}{\kappa_0} \right) \delta(E_2 - E_1 \pm \hbar\omega_{\mathrm{op}}), \tag{3.15}$$

and the correction factor is

$$G_{\mathrm{SL}}(q_\rho, q_z) = \frac{(q_\rho^2 + q_z^2) d}{2 q_\rho} \frac{\sinh(q_\rho d)}{\cosh(q_\rho d) - \cos(q_z d)} \times \int_{-d/2}^{d/2} g(s_1) ds_1 \int_{-d/2}^{d/2} g(s_2) ds_2 e^{-q_\rho |s_2 - s_1|} \times \cos[q_z (s_2 - s_1)]. \tag{3.16}$$

It can be verified that in the uniform limit $G_{\mathrm{SL}} \to 1$. Similarly, Eq. (2.13) holds for a multiple quantum well, where

$$W_{\mathrm{PO}}^{\mathrm{2D}}(q_\rho, q_z) = W_{\mathrm{PO}}^{\mathrm{3D}}(q_\rho, q_z = 0)[q_\rho G_{\mathrm{2D}}(q_\rho)] \tag{3.17}$$

and

$$G_{\mathrm{2D}}(q_\rho) = \tfrac{1}{2} \int_{-L/2}^{L/2} \rho(z_1) dz_1 \int_{-L/2}^{L/2} \rho(z_2) dz_2 e^{-q_\rho |z_2 - z_1|}. \tag{3.18}$$

Again, the quasi-2D result agrees with that derived previously by Price.[5]

IV. SOLUTION OF THE BOLTZMANN EQUATION FOR 2D, ISOTROPIC 3D, AND ANISOTROPIC 3D SYSTEMS

Having obtained generalized expressions for the transition rates in a superlattice, we now discuss the calculation of free-carrier mobilities using the Boltzmann equation. We will work within the single-particle picture, ignore collision broadening, and will employ the relaxation-time approximation. For a small external electric field and zero magnetic field, the Boltzmann equation in three dimensions may be written[13]

$$\mathbf{v}_1 \cdot \mathbf{F} = \int d\mathbf{k}_2 W^{\mathrm{3D,SL}}(\mathbf{q}) [(\mathbf{v}_1 \cdot \mathbf{F}) \tau(\mathbf{k}_1) - (\mathbf{v}_2 \cdot \mathbf{F}) \tau(\mathbf{k}_2)], \tag{4.1}$$

where $\mathbf{v} \equiv \nabla_k E(\mathbf{k})/\hbar$ is the velocity of state $\mathbf{k}$, $\mathbf{F}$ is the electric field, $W^{\mathrm{3D,SL}}(\mathbf{q})$ is the uniform 3D or superlattice transition rate for scattering from $\mathbf{k}_1$ to $\mathbf{k}_2$, and $\tau(\mathbf{k})$ is the momentum relaxation time.

For elastic scattering processes in an isotropic 3D system, $\tau(\mathbf{k})$ depends only on the magnitude of $\mathbf{k}$. Since conservation of energy then implies $\tau(\mathbf{k}_2) = \tau(\mathbf{k}_1)$, the relaxation times may be taken outside the integral and solution of the Boltzmann equation is trivial. For the isotropic 3D limit, one immediately obtains

$$\tau_{\mathrm{3D}}^{-1}(k_1) = \frac{k_1^2}{4\pi^2 \hbar v_1} \int_0^\pi d\theta \sin\theta (1 - \cos\theta) \left(\frac{W^{\mathrm{3D}}(q)}{\delta_E} \right), \tag{4.2}$$

where $q^2 = 2k_1^2(1 - \cos\theta)$.

However, in a system with cylindrical rather than spherical symmetry, τ depends on both k_ρ and k_z. If we take $\mathbf{F}$ to be in the plane and consider only intrasubband transitions, Eq. (4.1) is then

$$v_{\rho 1} = \frac{1}{(2\pi)^3} \int_{-\pi/d}^{\pi/d} dk_{z2} \int_0^{2\pi/a} k_{\rho 2} dk_{\rho 2} \int_0^{2\pi} d\gamma \, W^{\mathrm{SL}}(q_\rho, q_z) [v_{\rho 1} \tau(k_{\rho 1}, k_{z1}) - v_{\rho 2} \tau(k_{\rho 2}, k_{z2}) \cos\gamma], \tag{4.3}$$

where d is again the superlattice period, a is the lattice constant, γ is the angle in the plane between $\mathbf{k}_1$ and $\mathbf{k}_2$, $q_\rho^2 = 2k_{\rho 1}^2(1 - \cos\gamma)$, $q_z = k_{z2} - k_{z1}$, and umklapp processes have been neglected. In general, a closed-form solution of this equation is not possible. Various approaches have been discussed in connection with electron transport in the anisotropic conduction-band minima of germanium and silicon,[14–16] since those systems have the same cylindrical symmetry. The most general is probably that of Saso and Kasuya,[17] who solved Eq. (4.3) iteratively (see also Ref. 8). Unfortunately, we find that the iterative method is less useful in connection with the present problem whenever the dispersion is not well behaved. In particular, it does not converge well when k_ρ vs E at a given k_z is double-valued and the final states for elastic transitions occupy more than one region of the Brillouin zone. Such double-valued behavior frequently occurs in superlattice valence bands (e.g., see Fig. 1 below).

In order to be able to treat hole transport in superlattices with arbitrary dispersion relations, we have therefore employed an alternative approach. The relaxation time for a given energy and given occurrence of that energy j (when the dispersion is multivalued) is modeled by a power series in k_z. The coefficients in the power series are adjusted to give the best solution to the Boltzmann equation. We first perform the k_ρ integral in Eq. (4.3) by employing the energy-conservation δ function:

$$\delta(E_2 - E_1 \pm \hbar\omega_\Gamma) \rightarrow \sum_{j=1}^{J} \frac{\delta(k_{\rho 2} - k_{\rho 2}^j(k_{\rho 1}, k_{z1}, k_{z2}))}{\partial E_2/\partial k_{\rho 2}}, \tag{4.4}$$

where $k_{\rho 2}^j(k_{\rho 1}, k_{z1}, k_{z2})$ is the jth value of $k_{\rho 2}$ which satisfies energy conservation (when the dispersion is multivalued, it crosses the energy E_1 a total of J different times). The Boltzmann equation thus reduces to the form

$$v_{\rho 1} = \frac{2}{(2\pi)^3\hbar} \int_{-\pi/d}^{\pi/d} dk_{z2} \sum_{j=1}^{J} k_{\rho 2}^j \int_0^\pi d\gamma \left(\frac{W^{\mathrm{SL}}(q_\rho, q_z)}{\delta_E}\right) \left(\frac{v_{\rho 1}}{v_{\rho 2}^j}\tau(k_{\rho 1}, k_{z1}) - \tau(k_{\rho 2}^j, k_{z2})\cos\gamma\right). \tag{4.5}$$

As long as only elastic scattering is considered, the solution to this integral equation at a given energy E is decoupled from the solutions at all other energies, and by specifying E we can reduce by one the number of independent variables. Thus we seek a function $\tau_j(k_z)$, where it is not necessary to specify k_ρ^j since it is understood to be the jth value which yields the correct energy for the given k_z. Note that Eq. (4.5) may then be considered a set of N coupled equations, obtained by evaluating Eq. (4.5) at N of discrete values of k_{z1}.

To solve these equations, we expand the relaxation time as a power series in k_z:

$$\tau_j(k_z) = \sum_{m=0}^{M} a_{jm} k_z^m. \tag{4.6}$$

The problem is therefore reduced to one of obtaining the $J(M+1)$ coefficients a_{jm} which give the smallest least-squares errors in the N coupled equations. In regions where the dispersion is well behaved and $J = 1$ (usually appropriate for electrons and sometimes for holes), we find that $M = 3$ is generally adequate to assure 1% accuracy (as determined from the error and from the rapid convergence of relaxation times obtained for successively larger values of M). While the error is somewhat greater (as much as 30%) in regions where $J = 2$ or 3, the effect on the net mobility tends to be relatively small because those regions generally do not give dominant contributions to the total conductivity. The primary disadvantage of the method described is that it does not easily accommodate a generalization to inelastic scattering processes. However, even mobilities for optical-phonon scattering can usually be estimated with reasonable accuracy by considering only scattering-out and ignoring scattering-in processes [the term in Eq. (4.5) proportional to $\cos\gamma$], since the latter tend to be smaller because of symmetry considerations.[18] In the previous 2D and 3D literature, this procedure is much more common than the more difficult general solution of the inelastic Boltzmann equation by iterative or variational methods.

Once the relaxation time $\tau(k_\rho, k_z)$ has been determined from either Eq. (4.2) (3D) or Eq. (4.5) (SL), the mobility can be obtained from the relation $\mu^{\mathrm{3D,SL}} = \sigma/ne$, where n is the carrier concentration:

$$n = \frac{1}{\pi^2} \int_0^{\pi/d} dk_{z1} \int_0^{2\pi/a} k_{\rho 1} dk_{\rho 1} f_0(k_{\rho 1}, k_{z1}) \tag{4.7}$$

and σ is the total conductivity:

$$\sigma = \frac{e^2}{2\pi^2 k_B T} \int_0^{\pi/d} dk_{z1} \int_0^{2\pi/a} k_{\rho 1} dk_{\rho 1} f_0(1 - f_0) \times v_{\rho 1}^2 \tau(k_{\rho 1}, k_{z1}), \tag{4.8}$$

where $f_0(k_\rho, k_z) = 1/(1 + e^{[E(k_\rho, k_z) - E_F]/k_B T})$ is the equilibrium Fermi distribution function and E_F is the Fermi energy.

Although the preceding discussion has specifically considered the case of in-plane transport, the expressions can easily be modified to yield growth-direction mobilities (keeping in mind that the Boltzmann equation approach is inappropriate in the limit where k_z is not a good quantum number because the momentum relaxation time is much shorter than the time for tunneling between adjacent wells). This may be accomplished by replacing $v_{\rho 1}$ by v_{z1} and $v_{\rho 2}^j$ by v_{z2} everywhere they appear in Eqs. (4.5) and (4.8), and solving by the same method. It should be emphasized that nowhere in Eqs. (4.5)–(4.8) is it necessary to define an effective mass, which is an essential feature whenever the superlattice bands are highly nonparabolic. The expressions given are fully general with respect to the input of arbitrary, numerically derived $E(k_\rho, k_z)$.

We now briefly consider the analogous expressions for a quasi-2D free-carrier system. The Boltzmann equation [Eq. (4.1)] is unchanged except that the transition rate is replaced by the 2D form, $W^{\mathrm{2D}}(q_\rho)$, and it is understood that the integral $d\mathbf{k}_2$ is over two dimensions rather than three. As in the isotropic 3D case, the problem is simplified because the relaxation time depends only on k_ρ. Using the energy-conservation δ function to integrate $dk_{\rho 2}$, both τ terms can be removed from the integral and one obtains

$$\tau_{\mathrm{2D}}^{-1}(k_{\rho 1}) = \frac{k_{\rho 1}}{2\pi^2\hbar v_{\rho 1}} \int_0^\pi d\gamma \left(\frac{W^{2D}(q_\rho)}{\delta_E}\right)(1 - \cos\gamma). \tag{4.9}$$

Again, $\mu^{2D} = \sigma_s/n_s e$, where the sheet density and sheet conductivity are given by

$$n_s = \frac{1}{\pi} \int_0^{2\pi/a} k_{\rho 1} dk_{\rho 1} f_0(k_{\rho 1}) \tag{4.10}$$

and

$$\sigma_s = \frac{e^2}{2\pi k_B T} \int_0^{2\pi/a} k_{\rho 1} dk_{\rho 1} f_0(1 - f_0) v_{\rho 1}^2 \tau(k_{\rho 1}). \tag{4.11}$$

Note that in the multiple quantum well limit, one

has $n \rightarrow n_s/d$ and $\sigma \rightarrow \sigma_s/d$. With Eq. (2.12) and (2.13), these relations imply $\tau_{\mathrm{MQW}} \rightarrow \tau_{\mathrm{2D}}$ and $\mu^{\mathrm{MQW}} \rightarrow \mu^{\mathrm{2D}}$. The present formalism therefore provides a smooth bridge between the quasi-2D and the uniform 3D limits.

V. QUANTITATIVE COMPARISON OF QUASI-2D, ISOTROPIC 3D, AND SL MOBILITIES

In this section, we illustrate the effects of reduced dimensionality by quantitatively comparing in-plane mobilities obtained using the quasi-2D, isotropic 3D, and superlattice formalisms. As a test system, we consider the HgTe-CdTe superlattice whose lowest-order electron and hole subbands[19] are shown in Fig. 1. In this example, the electrons have significant dispersion in both k_ρ and k_z, but the mass is clearly quite anisotropic ($m_n^\rho \gg m_n^z$). For the holes, m_p^z is essentially infinite near the band extremum (the growth-direction dispersion for $k_\rho = 0$ is shown in the right panel of the figure), although a modest dispersion in k_z appears when k_ρ is increased somewhat (not shown in the figure). Hence hole mobilities calculated for the superlattice should be comparable but not strictly equal to those obtained in the quasi-2D limit. Note also that whereas the conduction-band dispersion in the plane is qualitatively similar to that in the bulk, the valence band is exceptionally nonparabolic. While m_p^ρ is just slightly larger than m_n^ρ at the top of the band, it becomes infinite and then negative (electronlike) at only slightly lower energies. Thus $k_\rho(E)$ is multivalued ($J = 3$) for energies between -38 and -45 meV, and there are three different **k** regions for which energy can be conserved in an elastic scattering process (see the discussion in Sec. IV). The Fermi level was evaluated numerically, using band structures for a number of T between 4.2 and 300 K and assuming a net acceptor concentration: $N_A - N_D = 3 \times 10^{14}$ cm^{-3} (these parameters correspond to a superlattice studied experimentally in Ref. 20). Our primary concern here is with contrasting the various dimensionality limits, although a separate work will discuss a more detailed HgTe-CdTe mobility calculations for comparison with experimental results. The present formalism is ideally suited for this because it can easily accommodate the numerical input of complicated band structures [dispersion relations for semimetallic HgTe-CdTe (Ref. 21) are even more complex than those shown in Fig. 1 for a nonzero gap].

We will approximate the wave-function distribution functions using the lowest-subband result for an infinite square well of width d_W:

$$g(s) \propto |\psi(s)|^2 \approx \begin{cases} \dfrac{2}{d_W} \cos^2\left(\dfrac{\pi s}{d_W}\right), & |s| \le d_W \\ 0, & |s| > d_W . \end{cases} \tag{5.1}$$

In general, the more exact functional forms obtained from numerical band-structure calculations depend on the penetration of the wave functions into the barriers, etc. However, the net mobility is not extremely sensitive to the details of $g(s)$ as long as the width of the distribution is accurately estimated and the wave function is confined primarily to the wells (which is the case for the example being considered, since the barriers are high and relatively thick).

For both electrons and holes, Figs. 2–5 illustrate $\mu^{\mathrm{SL}}/\mu^{\mathrm{2D}}$ and $\mu^{\mathrm{SL}}/\mu^{\mathrm{3D}}$, i.e., ratios of the superlattice mobilities to the quasi-2D and isotropic 3D values.[22] The various curves show dependences on temperature for each of the four mechanisms discussed in Sec. III. Phonon parameters have been taken from values which previously gave good agreement between theory and experiment for electron and hole mobilities in bulk HgTe.[23]

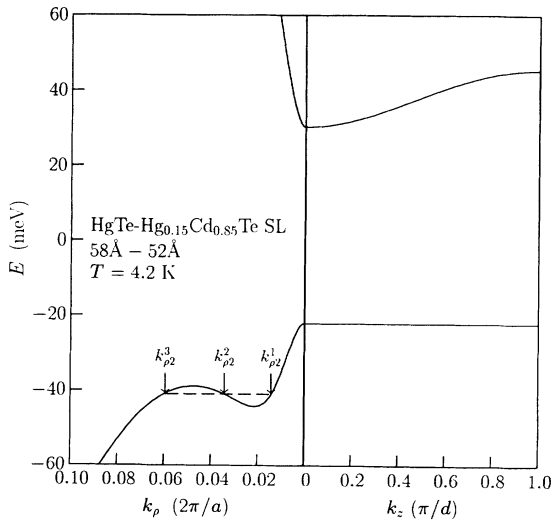

FIG. 1. Calculated band structure (Ref. 19) for a [100] $HgTe\text{-}Hg_{0.15}Cd_{0.85}Te\text{-}CdTe$ superlattice with well and barrier thicknesses $d_W = 58$ Å and $d_B = 52$ Å. For elastic processes with an initial energy of -41 meV, the arrows indicate three different final states for which energy can be conserved.

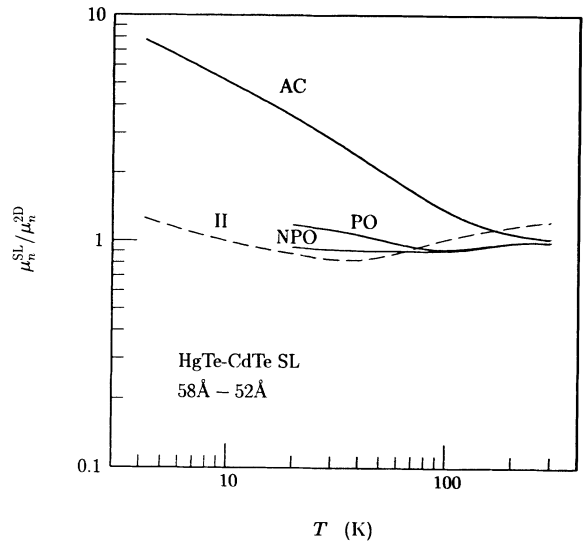

FIG. 2. Ratio of superlattice to 2D electron mobility. The solid curve is for the net mobility, while the dashed curves are for the various individual mechanisms: ionized impurity (II), acoustic-phonon (AC), nonpolar-optical-phonon (NPO), and polar-optical-phonon (PO).

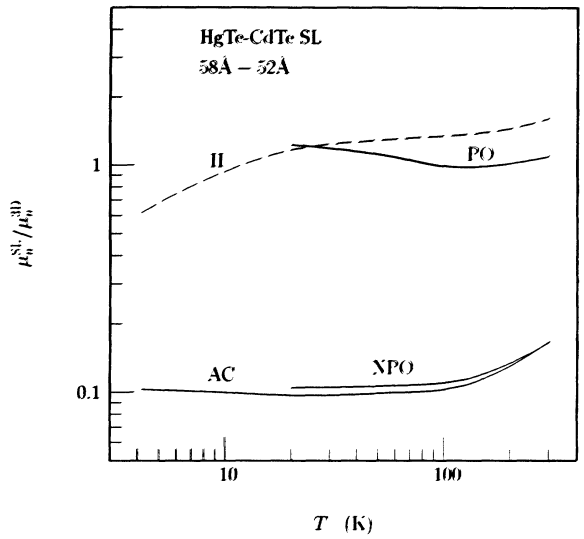

FIG. 3. Ratio of superlattice to isotropic 3D electron mobility. The solid curve is for the net mobility, while the dashed curves are for the various individual mechanisms.

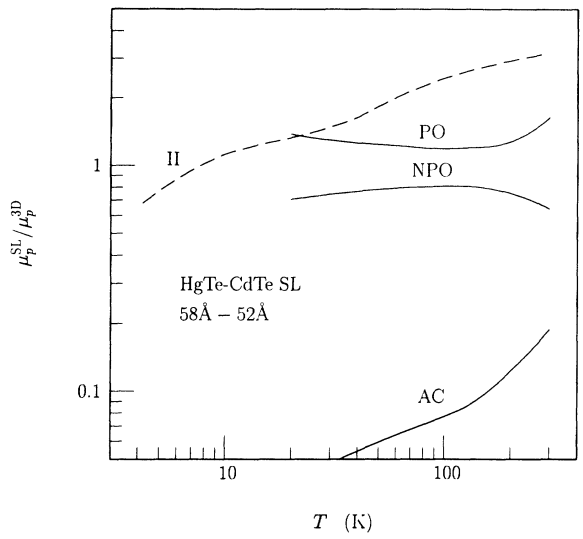

FIG. 5. Ratio of superlattice to isotropic 3D hole mobility. The solid curve is for the net mobility, while the dashed curves are for the various individual scattering mechanisms.

We begin by discussing acoustic-phonon scattering, since the transition rate is simplest for that mechanism and the effects of dimensionality are most easily understood. As has been noted by a number of previous authors:[5,12,24,25] $\mu^{2D} \ll \mu^{3D}$ at low temperatures, due primarily to the large qualitative effect of 2D confinement on the density of final states for scattering. Whereas this density goes as $k_1^2/v_1 \propto E^{1/2}$ in 3D [see Eq. (4.2)], it is independent of energy [$\propto k_{\rho 1} v_{\rho 1}/d_W$, from Eqs. (3.10) and (4.9)] in 2D because of the "flattening-out" of the dispersion in the third dimension. Thus for nondegenerate statistics: $\mu^{2D}/\mu^{3D} \propto d_W T^{1/2}$. The superlattice mobility generally falls somewhere in between, since for $m_n^\rho < m_n^z < \infty$, the density of final states is intermediate between those for the 2D and 3D limits.

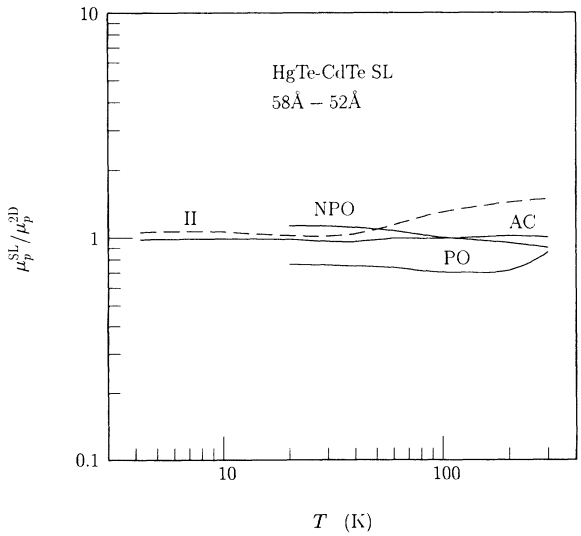

FIG. 4. Ratio of superlattice to 2D hole mobility. The solid curve is for the net mobility, while the dashed curves are for the various individual mechanisms.

However, apart from effects related to the densities of states, the nonuniformity of the distribution function in a superlattice leads to a further decrease of the mobility. Substitution of $g(s)$ from Eq. (5.1) into Eq. (3.8) yields $W_{AC}^{SL} = (3d/2d_W)W_{AC}^{3D}$. That is, even if the 3D and SL dispersion relations are taken to be identical, the superlattice scattering rate is larger and the mobility smaller by a factor of $3d/2d_W$ (in practice, the factor will be somewhat greater due to the larger growth-direction mass in the superlattice). Figures 2 and 3 confirm that μ_n^{SL} for acoustic-phonon scattering is intermediate between the 2D and 3D results, and that evaluating the mobility in either of those limits would lead to error by nearly an order of magnitude at $T = 4$ K. On the other hand, the hole mobility in the superlattice is well approximated by μ_p^{2D} (and quite poorly approximated by μ_p^{3D}) since the valence-band dispersion in Fig. 1 is nearly two dimensional.

Nonpolar-optical-phonon scattering is somewhat similar to acoustic-mode scattering, in that the transition rate has no explicit dependence on q and the corrections due to wave-function nonuniformity [Eq. (3.8)] are identical. However, whereas the low-temperature acoustic-phonon scattering rate is proportional to the density of states near the zone center, which is much larger in 2D than 3D (and intermediate in the SL), the NPO scattering rate depends on the density of states $\hbar\omega_{op}$ above the bottom of the band. This means that for the bands in Fig. 1, both of which have a miniband width ΔE less than $\hbar\omega_{op}$, one can scatter to final states spanning the entire Brillouin zone in k_z. Since the density of final states in the superlattice is nearly equal to that in 2D (even for electrons), both μ_n^{SL} and μ_p^{SL} are quite close to the corresponding quasi-2D results. However, it should be emphasized that this is not inevitable, since in a superlattice with $\Delta E > \hbar\omega_{op}$ (i.e., with thinner barriers), the allowed final states cover only a portion of the zone. Under those conditions, one would obtain $\mu_n^{SL} > \mu_n^{2D}$. In

the isotropic 3D calculation, which takes the dispersion along k_z to be the same as that along k_ρ, one clearly has a much smaller density of final states. This is particularly true of the electrons, for which μ_n^{3D} is nearly an order of magnitude larger than μ_n^{SL}. The effect is somewhat smaller for holes ($\mu_p^{3D}/\mu_p^{SL} \approx 2$) because of the strong nonparabolicity of m_p^ρ.

The effect of dimensionality on polar-optical-phonon scattering is more complicated, due to the explicit $1/(q_\rho^2+q_z^2)$ dependence in the transition rate [see Eq. (3.15)]. This factor favors a small m^z, since one can then achieve the same energy transfer with a smaller q_z. The ratio μ^{2D}/μ^{3D} can thus be either greater than or less than unity, depending on d_W.[26] Whereas the density-of-states factor favors μ^{3D} being larger, Eqs. (3.17) and (3.18) show that W_{PO}^{2D}/W_{PO}^{3D} decreases with increasing d_W (for which $q_\rho|z_2 - z_1|$ tends to be larger). The effect is more pronounced for holes than for electrons, since the thermal average of q_ρ is greater. Thus in the present example, $\mu_p^{2D}/\mu_p^{3D} \approx 2$ while $\mu_n^{2D}/\mu_n^{3D} \approx 1$. The mobility in the superlattice lies between the two limits for both electrons and holes, but for electrons this means that all three mobilities are equal to within 20%.

Finally, ionized impurity scattering is somewhat analogous to polar-optical-phonon processes, in that the interaction potential has an inverse dependence on q [see Eq. (3.4)]. Due to competition between this factor and the density-of-states considerations, μ^{2D} can again be either greater than or less than μ^{3D}, with μ_{SL} usually lying in between. As pointed out in Sec. III, the same 3D screened Coulomb scattering potential was used in all three calculations, since that form is quite accurate when the net doping level is light to moderate. However, we emphasize that had the quasi-2D scattering potential for single-period structures[1,4] been employed in obtaining μ^{2D}, the apparent effects of dimensionality would have been far greater,[27] since interwell scattering and screening dominate when $q_{s3}^{-1} > d$. A detailed discussion of interwell effects on ionized impurity scattering will be given in a separate work,[10] which also considers the heavy-doping regime[28] where one must employ the general solution to the anisotropic Poisson's equation rather than the isotropic 3D potential.

VI. CONCLUSIONS

In the preceding sections, we have presented a comprehensive single-particle treatment of free-carrier transport in superlattices. A key feature is the general incorporation of both the anisotropy of the dispersion relations and the nonuniformity of the wave-function distribution functions. While the superlattice "environment" may be thought of as an intermediate regime bridging the quasi-2D and uniform (but anisotropic) 3D limits, it is clear that previous transport formalisms developed for those limits are not applicable to the more general problem.

Scattering transition rates have been derived on the basis of a weighted potential, which accounts for the overlap of the actual potential with the wave-function distribution function. Specific expressions for scattering by ionized impurities and acoustic-, nonpolar-optical-, and polar-optical-phonon modes reduce to previously derived quasi-2D forms in the multiple-quantum-well limit. Although we have explicitly considered only intrasubband processes, generalization to interband scattering would be straightforward. Similarly, whereas the discussion has focused on two-component superlattices with flat wells and barriers, the derived expressions are sufficiently general to account for more complicated multiperiod structures with arbitrary electron and hole wave-function distributions.

Solution of the Boltzmann equation for arbitrary anisotropic dispersion relations and input scattering rates has been discussed, along with expressions for obtaining mobilities both in the plane of the superlattice and in the growth direction. For the example of a finite-gap HgTe-CdTe superlattice, in-plane mobilities from the general calculation have been compared with results for the quasi-2D and isotropic 3D limits. We frequently find that the superlattice mobility cannot be accurately approximated by either of the two limiting values, although it generally lies between them. It should finally be emphasized that while we have explicitly considered solution of the anisotropic Boltzmann equation in the low-field limit (Sec. IV), the transition rates derived in Secs. II and III are equally applicable to high-field transport in superlattices.

ACKNOWLEDGMENTS

We thank L. R. Ram-Mohan for the use of his superlattice band-structure software. This research was supported in part by the Office of Naval Research and in part by the Stategic Defense Initiative/Innovative Science and Technology.

---

*Present address: IBM Thomas J. Watson Research Center, Yorktown Heights, NY 10598.

[1] T. Ando, A. B. Fowler, and F. Stern, Rev. Mod. Phys. **54**, 437 (1982).

[2] J. J. Harris, J. A. Pals, and R. Woltjer, Rep. Prog. Phys. **52**, 1217 (1989).

[3] Several theoretical and experimental papers with titles referring to "superlattices" have in fact treated multiple quantum wells [e.g., S. Mori and T. Ando, J. Phys. Soc. Jpn. **48**, 865 (1980); R. Dingle, H. L. Störmer, A. C. Gossard, and W. Wiegmann, Appl. Phys. Lett. **33**, 665 (1978)]. Also discussed have been superlattices with barriers thick enough that the wells interact only weakly. In such cases the transport results have generally been analyzed in terms of the quasi-2D theory (e.g., Ref. 27).

[4] F. Stern and W. E. Howard, Phys. Rev. **163**, 816 (1967).

[5] P. J. Price, Ann. Phys. **133**, 217 (1981).

[6] M. Artaki and K. Hess, Superlatt. Microstruct. **1**, 489

(1985).
[7] J. F. Palmier and A. Chomette, J. Phys. **43**, 381 (1982).
[8] G. J. Warren and P. N. Butcher, Semicond. Sci. Technol. **1**, 133 (1986).
[9] For cgs and a dimensionality D, the potential has units $\mathrm{eV\,cm}^D$, Ω has units cm^D, and W_Γ has units cm^D/s.
[10] J. R. Meyer, D. J. Arnold, F. J. Bartoli, and C. A. Hoffman (unpublished).
[11] K. Seeger, *Semiconductor Physics* (Springer-Verlag, New York, 1973).
[12] B. K. Ridley, J. Phys. C **15**, 5899 (1982).
[13] J. M. Ziman, *Princples of the Theory of Solids*, 2nd ed. (Cambridge University Press, London, 1972), Chap. 7.
[14] C. Herring and E. Vogt, Phys. Rev. **101**, 944 (1956).
[15] A. G. Samoilovich, I. Ya. Korenblit, I. V. Dakhovskii, and V. D. Iskra, Fiz. Tverd. Tela (Leningrad) **3**, 3285 (1961) [Sov. Phys. Solid State **3**, 2385 (1962)].
[16] J. B. Krieger, T. Meeks, and E. Esposito, Phys. Rev. B **5**, 1499 (1972).
[17] T. Saso and T. Kasuya, J. Phys. Soc. Jpn. **49**, 578 (1980).
[18] When calculating mobilities for nonpolar- and polar-optical-phonon scattering using the relaxation-time approximation, it is generally more accurate to ignore the scattering-in term altogether.
[19] J. R. Meyer, D. J. Arnold, C. A. Hoffman, F. J. Bartoli, and L. R. Ram-Mohan, J. Vac. Sci. Technol. B **9**, 1818 (1991).
[20] C. A. Hoffman, J. R. Meyer, E. R. Youngdale, J. R. Lindle, F. J. Bartoli, K. A. Harris, J. W. Cook, Jr., and J. F. Schetzina, Phys. Rev. B **37**, 6933 (1988).
[21] C. A. Hoffman, J. R. Meyer, F. J. Bartoli, J. W. Han, J. W. Cook, Jr., J. F. Schetzina, and J. N. Schulman, Phys. Rev. B **39**, 5208 (1989).
[22] The same Fermi level was employed in all three calculations, which is somewhat artificial since the density of states depends fairly strongly on dimensionality. However, it assures that the contrasts observed in Figs. 2–5 are actually due to dispersion and nonuniformity effects, rather than resulting from differing effective masses in different regions of the Brillouin zone.
[23] J. R. Meyer, C. A. Hoffman, F. J. Bartoli, J. M. Perez, J. E. Furneaux, R. J. Wagner, R. J. Koestner, and M. W. Goodwin, J. Vac. Sci. Technol. A **6**, 2775 (1988).
[24] P. Kaw, Phys. Rev. Lett. **21**, 539 (1968).
[25] K. Hess, Appl. Phys. Lett. **35**, 484 (1979).
[26] D. Chattopadhyay, Phys. Rev. B **33**, 7288 (1986).
[27] W. T. Masselink, Phys. Rev. Lett. **66**, 1513 (1991).
[28] C. A. Hoffman, J. R. Meyer, F. J. Bartoli, Y. Lansari, J. W. Cook, Jr., and J. F. Schetzina, Phys. Rev. B **44**, 8376 (1991).